

CASE FILE
COPY

N 62 62762
RM E54F17a

2181

NACA

RESEARCH MEMORANDUM

NOTE ON PERFORMANCE OF AIRCRAFT EJECTOR
NOZZLES AT HIGH SECONDARY FLOWS

By Fred D. Kochendorfer

Lewis Flight Propulsion Laboratory
Cleveland, Ohio

NATIONAL ADVISORY COMMITTEE
FOR AERONAUTICS
WASHINGTON

August 27, 1954
Declassified June 20, 1957

NACA RM E54F17a

NATIONAL ADVISORY COMMITTEE FOR AERONAUTICS

RESEARCH MEMORANDUM

NOTE ON PERFORMANCE OF AIRCRAFT EJECTOR

NOZZLES AT HIGH SECONDARY FLOWS

By Fred D. Kochendorfer

SUMMARY

An ejector analysis employing simple one-dimensional flow theory was conducted in order to obtain quantitative estimates of the maximum values of secondary flow and secondary pressure which would permit operation with a choked primary nozzle.

The results show that for an ejector having a convergent shroud the maximum flow and pressure values can be much less than those for a cylindrical ejector, the discrepancy increasing for larger amounts of convergence. Comparison of the theoretical results with existing experimental data indicates good agreement for weight-flow values and fair agreement for pressure values.

INTRODUCTION

In recent ejector tests the flow coefficient of the primary nozzle was found to decrease sharply as the secondary flow was increased beyond some critical value. An obvious explanation was that the static pressure in the secondary stream in the region of the primary-nozzle exit must have been sufficiently high to unchoke the nozzle. With a conical ejector, it was clear that this could happen for values of secondary total pressure lower than those of the primary, but quantitative estimates of these critical secondary pressures were not available. The purpose of this investigation was to study the performance of ejectors at high weight-flow ratios to obtain values of the critical ejector pressure ratio and weight-flow ratio. An analysis employing simple one-dimensional flow theory was conducted. The results are compared with existing experimental data.

SYMBOLS

The following symbols are used in this report:

A	area
A/A^*	$\frac{1}{M} \sqrt{\left[\frac{2}{\gamma + 1} \left(1 + \frac{\gamma - 1}{2} M^2 \right) \right]^{\frac{\gamma + 1}{\gamma - 1}}}$
A_S	shroud exit area
A'_S	secondary flow area at shroud entrance
a	ejector area ratio, A_S/A_p
b	primary area ratio, A_1/A_p
C_D	nozzle discharge coefficient
C'_D	nozzle discharge coefficient with zero secondary flow
D	diameter
L	shroud length
M	Mach number
m	molecular weight
P	total pressure
p	static pressure
T	total temperature
w	weight flow
α	secondary area ratio, $\frac{A'_S}{A_S - A_p}$
γ	specific heat ratio
μ	molecular weight ratio, m_s/m_p
τ	temperature ratio, T_s/T_p
ω	weight-flow ratio, w_s/w_p

Subscripts:

- p primary stream at nozzle exit
 s secondary stream at nozzle exit
 0 jet ambient
 1 primary stream at shroud exit
 2 secondary stream at shroud exit

Superscript:

- * station at which $M = 1.0$

ANALYSIS

The effect of secondary flow on the performance of the primary nozzle will be discussed first for the cylindrical ejector sketched in figure 1. It has been shown (e.g., refs. 1 and 2) that at low values of the ejector pressure ratio P_s/P_p (curve I) the primary stream accelerates supersonically and expands upon leaving the nozzle. Because of the reduced flow area, the secondary stream also accelerates as it moves into the shroud and the static pressure along the boundary between the two streams decreases. Both streams accelerate until the secondary Mach number equals unity. (In all the discussion which follows, it will be assumed that the ambient pressure p_0 is low enough to choke the secondary stream at the shroud exit.) The secondary flow is limited by the expansion of the primary stream and can be increased only by increasing the ejector pressure ratio P_s/P_p .

When the ejector pressure ratio is increased to a value of unity, $M_s = M_p$, no primary expansion occurs, and the weight-flow ratio is such that $\omega\sqrt{\tau/\mu} = a - 1$, where ω is the secondary to primary weight-flow ratio, τ/μ is the quantity which corrects for the temperature and molecular weight ratios, and a is the area ratio A_s/A_p (curve II). The shroud static pressure is constant. Further increases in P_s unchoke the primary stream, and the roles of the two streams are interchanged. Thus, for the cylindrical ejector, the minimum weight-flow ratio and ejector pressure ratio which can unchoke the primary nozzle are $a - 1$ and unity, respectively.

The case of a hypothetical ejector having a very large amount of convergence (fig. 2) is next considered. Since the secondary flow area

at the primary-nozzle exit is much greater than $A_S - A_p$, the secondary Mach number M_s must be very small. Then, since the secondary Mach number at the shroud exit is equal to unity, the ratio of the static pressure at the shroud exit to that at the primary nozzle exit, with isentropic

flow assumed, must be approximately $\left(\frac{2}{\gamma+1}\right)^{\frac{\gamma}{\gamma-1}}$ or 0.528 for $\gamma = 1.4$. For values of the ejector pressure ratio lower than 0.528, the primary stream expands from the nozzle into a region of essentially constant pressure (curve a). Then, as the stream is about to leave the shroud, the reduction in pressure resulting from acceleration of the secondary stream causes further expansion of the primary stream.

At an ejector pressure ratio of 0.528 (curve II), the primary nozzle is just choked and the primary stream does not expand until just before it reaches the shroud exit. The exit primary Mach number M_1 is 1.47, corresponding to a pressure ratio of (0.528 in the nozzle) \times (0.528 in the shroud) = 0.280. The ratio of the area of the primary stream at the shroud exit to that at the nozzle exit A_1/A_p is 1.164; the flow area for the secondary stream at the shroud exit is thus $A_2 = A_S - A_1$ or $A_2 = A_p(a - 1.164)$, and the weight-flow ratio is $\omega\sqrt{\tau/\mu} = \frac{P_s}{P_p} \frac{A_2}{A_p} = 0.528(a - 1.164)$. For values of the ejector pressure ratio above 0.528, the nozzle is unchoked, the primary stream being throttled by the secondary near the shroud exit (curve III). The values of weight-flow ratio and ejector pressure ratio which unchoke the primary nozzle are therefore 0.528 $(a - 1.164)$ and 0.528, respectively. The ejector pressure ratio which unchokes the nozzle is therefore about half that for a cylindrical ejector; however, the weight flow which unchokes the nozzle may be much less than half that for a cylindrical ejector if the area ratio is small. It is interesting to note that for the convergent ejector, if the area ratio is less than 1.164, the nozzle cannot be choked for any nonzero secondary flow. Of course, it should be recognized that the preceding values must be considered as approximations in that they were obtained with the assumption of isentropic flow and no mixing between the two streams.

In general, the critical values for the conical ejector (fig. 3) lie somewhere between those of the two previous cases. The secondary flow area at the nozzle exit A'_S is greater than $A_S - A_p$, but not as great as in the previous hypothetical case. Let the ejector area ratio $\frac{A'_S}{A_p} = a$, the secondary area ratio $\frac{A'_S}{(A_S - A_p)} = \alpha$, and $A_1/A_p = b$. Then,

$$A_2/A_p = a - b \quad (1)$$

and

$$A_2/A'_S = \frac{a - b}{(a - 1) \alpha} \quad (2)$$

Also, let $w_s/w_p = \omega$, $T_s/T_p = \tau$, and $m_s/m_p = \mu$.

For one-dimensional flow the shroud-exit pressure must be uniform, that is,

$$P_2 = P_1 \quad (3)$$

At the nozzle exit, the secondary static pressure can, of course, be less than the primary static pressure if the nozzle is choked. However, since this analysis will be concerned only with those cases for which the nozzle is just choked or is unchoked, the static pressure of both streams must be equal; that is,

$$P_p = P_s \quad (4)$$

In order to obtain quantitative results, an assumption must be made regarding the loss in total pressure between the nozzle and the shroud exit for each stream. For short shrouds, mixing and friction losses should be small. Secondary losses should therefore be small. Likewise, primary losses can be small if the Mach numbers within the shroud do not become too great. For lack of better information, it will be assumed that both streams are isentropic. Then, since $P_1 = P_p$, $A_1^* = A_p^*$, $P_2 = P_s$, and $A_2^* = A_s^*$,

$$P_1/P_p = (p/P)_1/(p/P)_p \quad (5)$$

and

$$b = (A/A^*)_1/(A/A^*)_p \quad (6)$$

Also, since $M_2 = 1$,

$$P_2/P_s = \left(\frac{2}{\gamma_s + 1} \right)^{\frac{\gamma_s}{\gamma_s - 1}} / (p/P)_s \quad (7)$$

and

$$\frac{a - b}{\alpha(a - 1)} = 1/(A/A^*)_s \quad (8)$$

Now, since w_2 must equal w_s ,

$$\frac{w_s}{w_p} = \frac{w_2}{w_p} = \frac{A_2}{A_p} \sqrt{\frac{\gamma_s}{\gamma_p}} \sqrt{\left(\frac{2}{\gamma_{s+1}}\right)^{\frac{\gamma_{s+1}}{\gamma_s-1}}} \sqrt{\left(\frac{\gamma_{p+1}}{2}\right)^{\frac{\gamma_{p+1}}{\gamma_p-1}}} \sqrt{\frac{m_s}{m_p}} \sqrt{\frac{T_p}{T_s}} \frac{P_2}{P_p} (A/A^*)_p$$

or with equation (1)

$$\omega \sqrt{\tau/\mu} = (a - b) \sqrt{\frac{\gamma_s}{\gamma_p}} \sqrt{\left(\frac{2}{\gamma_{s+1}}\right)^{\frac{\gamma_{s+1}}{\gamma_s-1}}} \sqrt{\left(\frac{\gamma_{p+1}}{2}\right)^{\frac{\gamma_{p+1}}{\gamma_p-1}}} P_s/P_p (A/A^*)_p \quad (9)$$

These equations can be solved as follows:

(a) Choose values for M_p and M_s . The value for M_p determines the nozzle discharge coefficient: $C_D = 1/(A/A^*)_p$.

(b) Find $(p/P)_p$, $(A/A^*)_p$, $(p/P)_s$, and $(A/A^*)_s$.

(c) Then from equation (4), $P_s/P_p = (p/P)_p/(p/P)_s$; and from equations (3), (4), (5), and (7), $(p/P)_1 = \left(\frac{2}{\gamma_{s+1}}\right)^{\frac{\gamma_s}{\gamma_s-1}} \frac{P_s}{P_p}$.

(d) Find M_1 and $(A/A^*)_1$.

(e) Then, using equations (6) and (9), find b and $\frac{\omega \sqrt{\tau/\mu}}{a - b}$.

Calculations were made for $\gamma_p = \gamma_s = 1.4$ with this procedure. The resulting values for $\frac{\omega \sqrt{\tau/\mu}}{a - b}$ and b are presented in figure 4 and those for P_s/P_p in figure 5. It can be seen that the curves for each value of M_s end at the point $M_s = M_p$. This was done to avoid the anomaly $P_s/P_p > 1$ (see fig. 5). The curves can be used with equation (8) to obtain a solution for any desired value of the ejector area ratio a . Typical solutions are presented in figure 6 for ejector area ratios of 1.1 and 1.4. The weight-flow parameter is plotted as a function of secondary area ratio for several values of M_p and M_s . In general, increasing α at constant M_p (i.e., at constant nozzle discharge coefficient) decreases the weight-flow ratio; or, in other words, if the

weight-flow ratio is fixed, increasing α will decrease the discharge coefficient. In figure 6(a) there is no solution for $M_p = 1.0$ for values of α greater than unity. This, of course, is in accord with the previous result that for a convergent ejector having an area ratio less than 1.164, the primary nozzle cannot be choked for nonzero secondary flow.

Curves obtained from the values for $M_p = 1.0$ for a series of ejector area ratios are plotted in figure 7. The figure therefore represents the maximum flow for which the nozzle is choked as a function of the two area ratios α and a . It can be seen that the curves for all values of α lie between the extremes established previously. As α decreases from infinity to a value of about 2.5, the weight-flow parameter remains essentially constant. Further reductions, however, increase the weight flow appreciably.

A point of interest is that two values of the weight-flow parameter exist for $\alpha \leq 1.0$. The upper curve for $\alpha = 1.0$ has been shown to represent the cylindrical ejector; the lower values can perhaps be best explained by considering a particular case. Consider an ejector having $a = 1.4$ and $\alpha = 1.0$. The lower value of the weight-flow parameter corresponding to $M_p = 1.0$ is 0.21 and M_s is approximately 0.55 (fig. 6(b)). Calculations for the shroud area distribution, again with the assumption that the static pressures of the two streams are equal and the flow is isentropic, give the results of figure 8(a). The primary, secondary, and total flow areas are plotted as functions of M_p or M_s , or both. The primary flow area increases from the nozzle to the shroud exit and the secondary area decreases. The total area, however, first decreases, then increases. The lower curve for $\alpha = 1$ in figure 7 therefore represents convergent-divergent ejectors having shroud exit and entrance areas that are equal.

A question now arises as to the area distribution for values of α other than unity. An example of this case is an ejector having $a = 1.4$, $M_s = 0.2$, and (from fig. 6(b)) $\alpha = 1.85$. The area distribution is given in figure 8(b). The total area decreases rapidly at first, then increases, and the exit area, although smaller than that at the entrance, is larger than some intermediate areas. This ejector must therefore be of the type having a convergent-divergent shroud and is not truly conical. A conclusion which also follows is that for a conical ejector, the area distribution is such that shock losses cannot be avoided and the flow cannot be isentropic.

COMPARISON WITH EXPERIMENT

An idea of the error involved in assuming isentropic flow for a conical ejector can be had by comparing theoretical and experimental

results. In figure 9 discharge coefficient ratio and ejector pressure ratio are presented as functions of weight-flow parameter for a series of conical ejectors. The discharge coefficient ratio, defined as the ratio of the nozzle discharge coefficient with secondary flow to that with zero secondary flow, was plotted in order to obtain a better comparison. The curves represent the theory. The experimental data points were obtained from references 3, 4, and unpublished NACA data. Since in references 3 and 4 values of the discharge coefficient were not included, the original data were used to compute the points of figure 9(a). In general, good agreement is obtained with respect to discharge coefficient; the theory correctly evaluates the maximum flow for which the nozzle is choked and the slope of the curve for unchoked operation. However, only fair agreement is obtained for ejector pressure ratio. In figure 9(a), the curves are approximately parallel but are displaced by a value of about 0.08; in figure 9(b), the slopes are different. The discrepancy may result from the fact that the average primary and secondary total pressures are difficult to measure accurately or from the inadequacies of the theory, or both.

An additional comparison obtained from the data of reference 5 is presented in figure 10. The data are for the semicylindrical ejector shown in the sketch. Although the aft portion of the shroud is cylindrical, the section near the nozzle is conical. Agreement between experiment and theory is about the same as that noted for the conical ejector.

CONCLUDING REMARKS

Theoretical considerations have shown that for an ejector having a convergent shroud the maximum weight-flow ratio and ejector pressure ratio which permit operation with a choked primary nozzle can be much less than the corresponding values for a cylindrical ejector, the discrepancy increasing for larger amounts of convergence. Comparison of experimental results with those of a simple one-dimensional analysis indicated good agreement for the value of the maximum weight-flow ratio and for the slope of the discharge coefficient curve, but only fair agreement for values of ejector pressure ratio.

Lewis Flight Propulsion Laboratory
National Advisory Committee for Aeronautics
Cleveland, Ohio, July 2, 1954

REFERENCES

1. Kochendorfer, Fred D., and Rousso, Morris D.: Performance Characteristics of Aircraft Cooling Ejectors Having Short Cylindrical Shrouds. NACA RM E51E01, 1951.
2. Kochendorfer, Fred D.: Effect of Properties of Primary Fluid on Performance of Cylindrical Shroud Ejectors. NACA RM E53L24a, 1954.
3. Greathouse, W. K., and Hollister, D. P.: Preliminary Air-Flow and Thrust Calibrations of Several Conical Cooling-Air Ejectors with a Primary to Secondary Temperature Ratio of 1.0. I - Diameter Ratios of 1.21 and 1.10. NACA RM E52E21, 1952.
4. Greathouse, W. K., and Hollister, D. P.: Preliminary Air-Flow and Thrust Calibrations of Several Conical Cooling-Air Ejectors with a Primary to Secondary Temperature Ratio of 1.0. II - Diameter Ratios of 1.06 and 1.40. NACA RM E52F26, 1952.
5. Gorton, Gerald C.: Pumping and Drag Characteristics of an Aircraft Ejector at Subsonic and Supersonic Speeds. NACA RM E54D06, 1954.

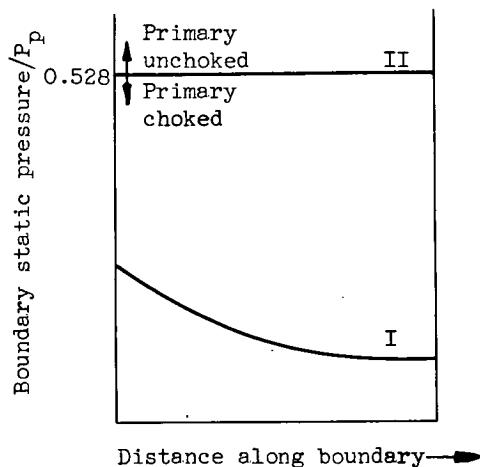
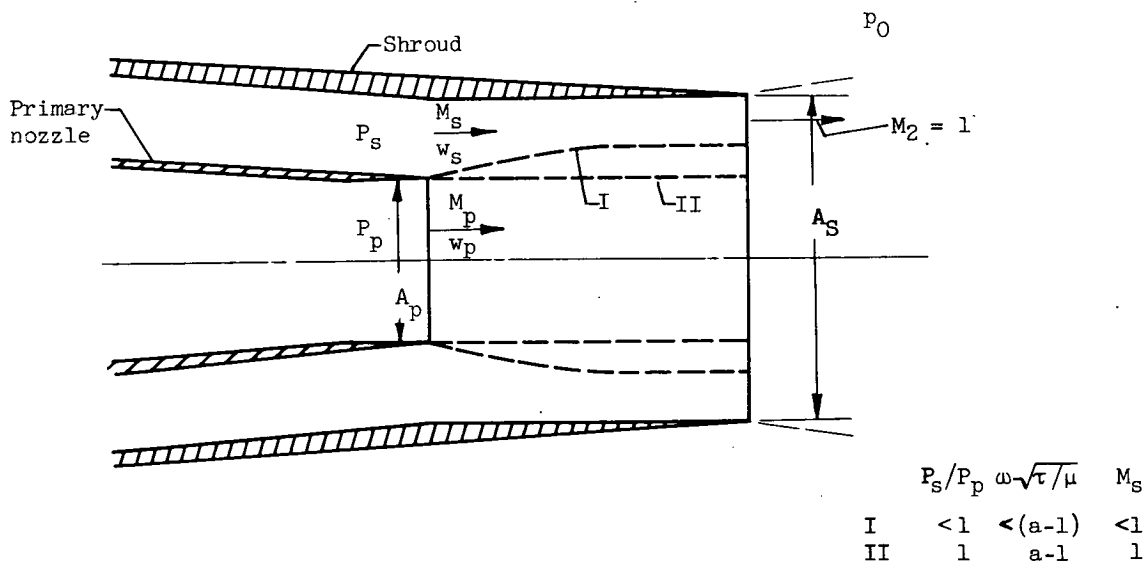


Figure 1. - Cylindrical ejector.

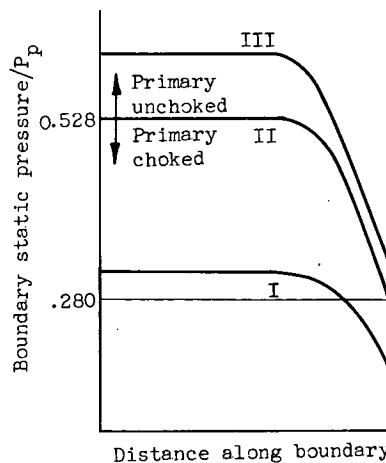
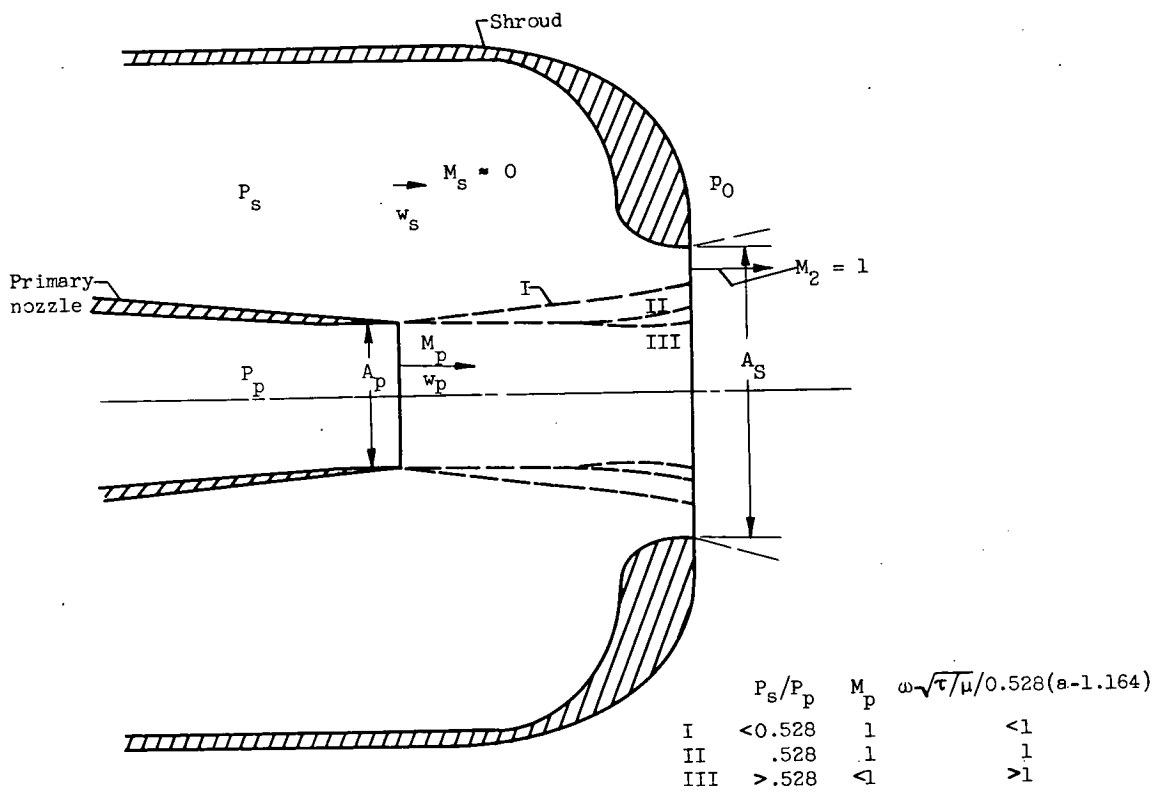


Figure 2. - Convergent ejector.

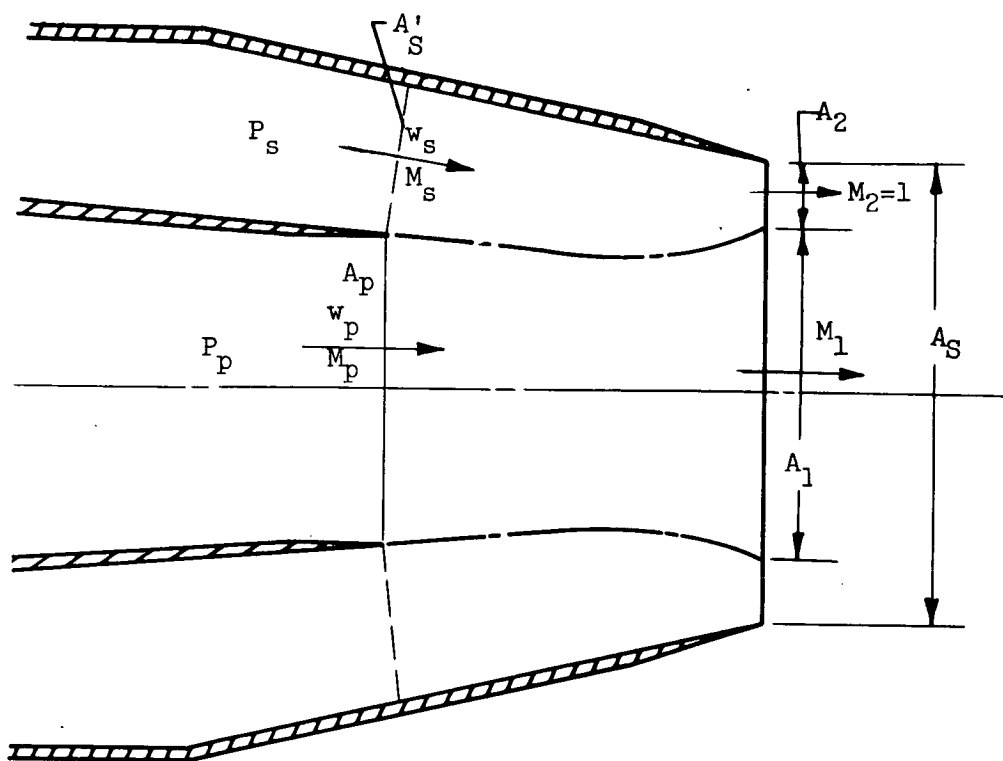


Figure 3. - Conical ejector.

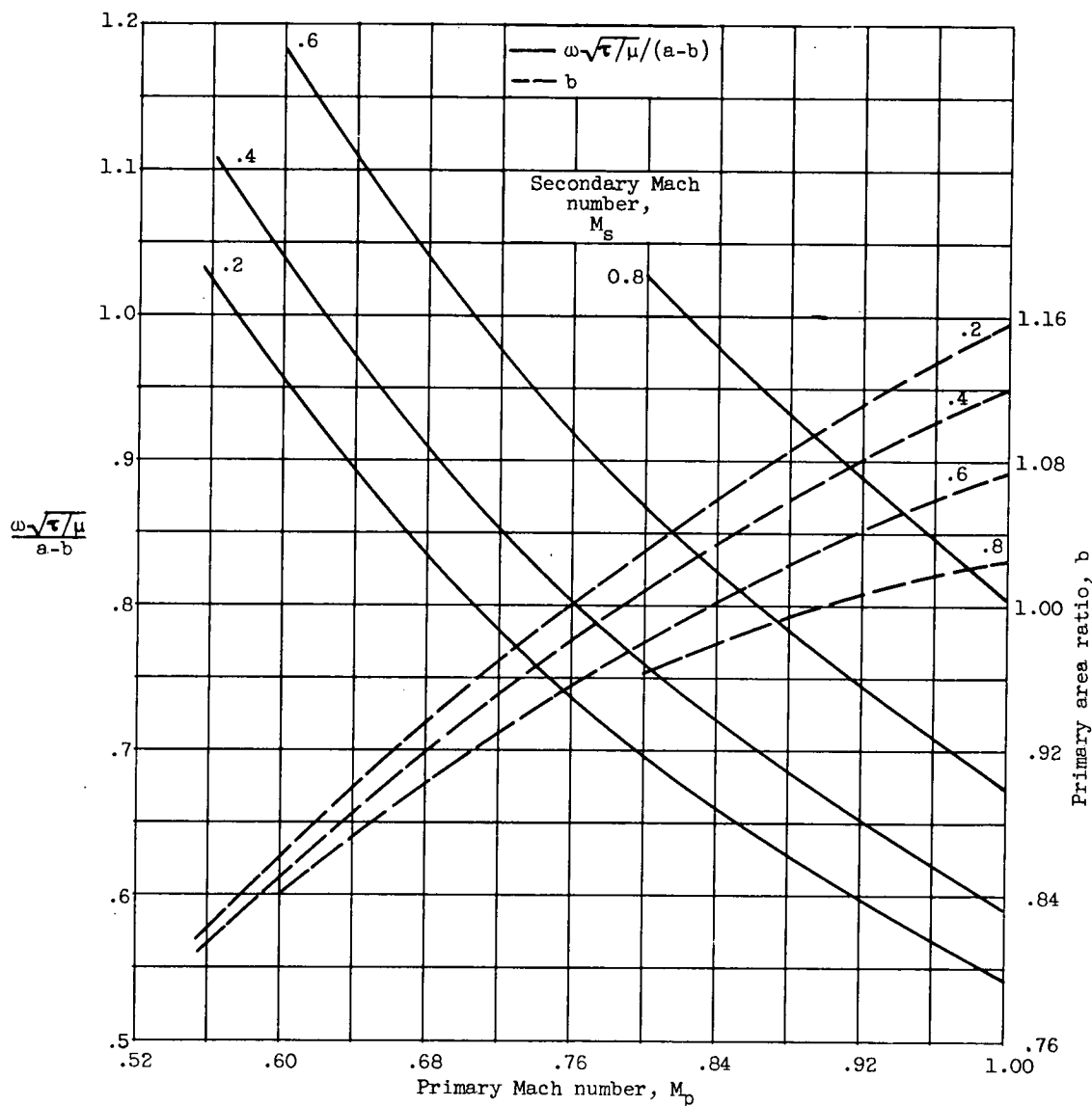


Figure 4. - Variation of $\frac{\omega\sqrt{\tau/\mu}}{a-b}$ and primary area ratio with primary Mach number for several values of secondary Mach number ($\gamma_p = \gamma_s = 1.4$).

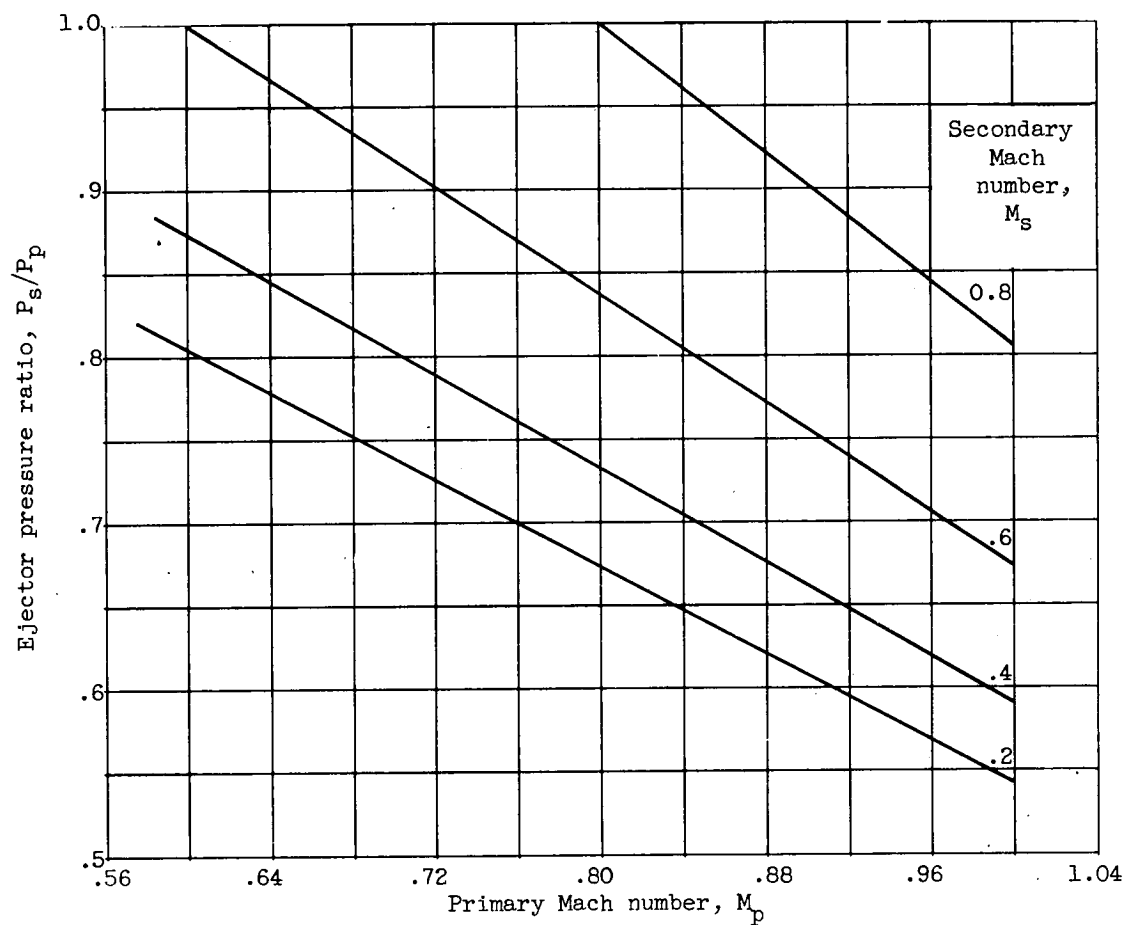


Figure 5. - Variation of ejector pressure ratio with primary Mach number for several values of secondary Mach number ($\gamma_p = \gamma_s = 1.4$).

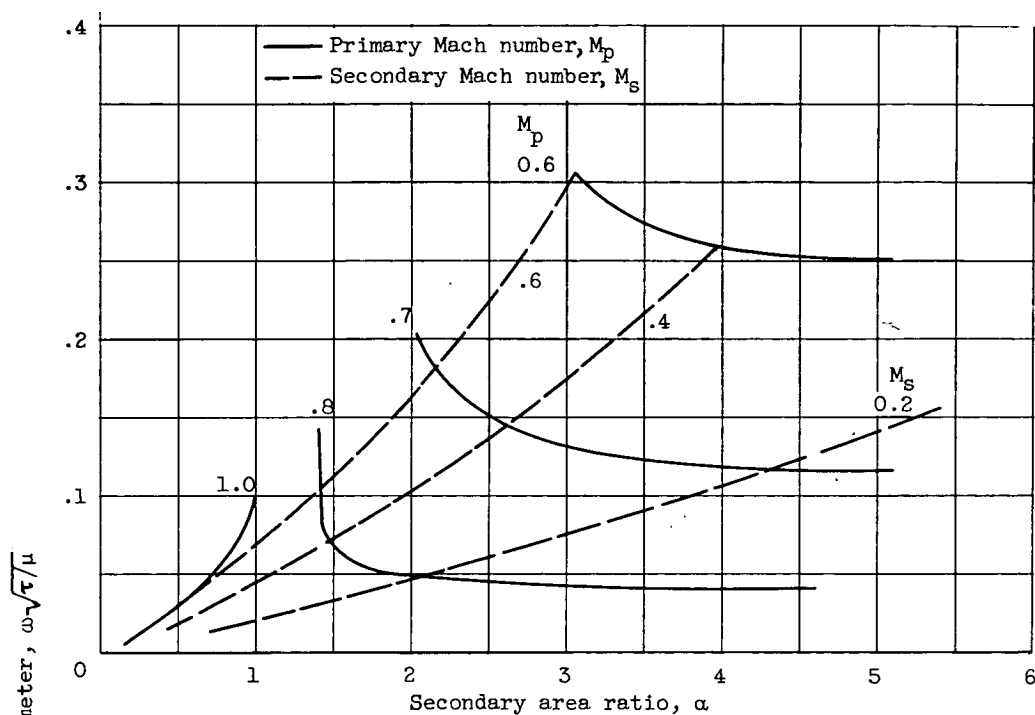
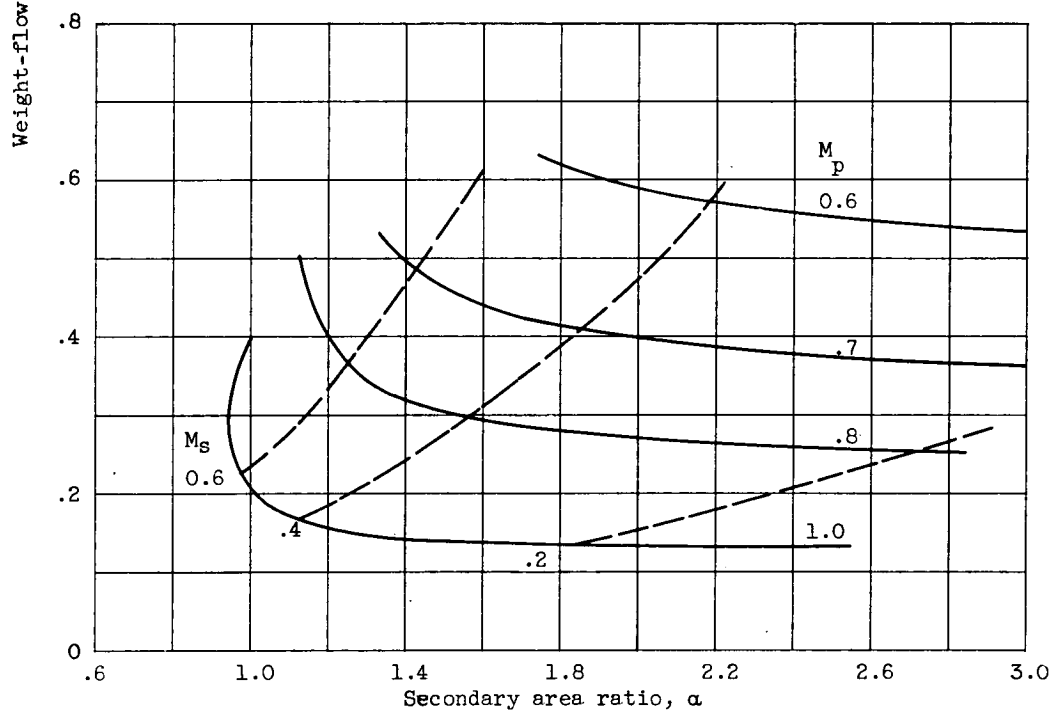
(a) Ejector area ratio, a , 1.1.(b) Ejector area ratio, a , 1.4.

Figure 6. - Weight flow as a function of secondary area ratio for several values of primary and secondary Mach number.

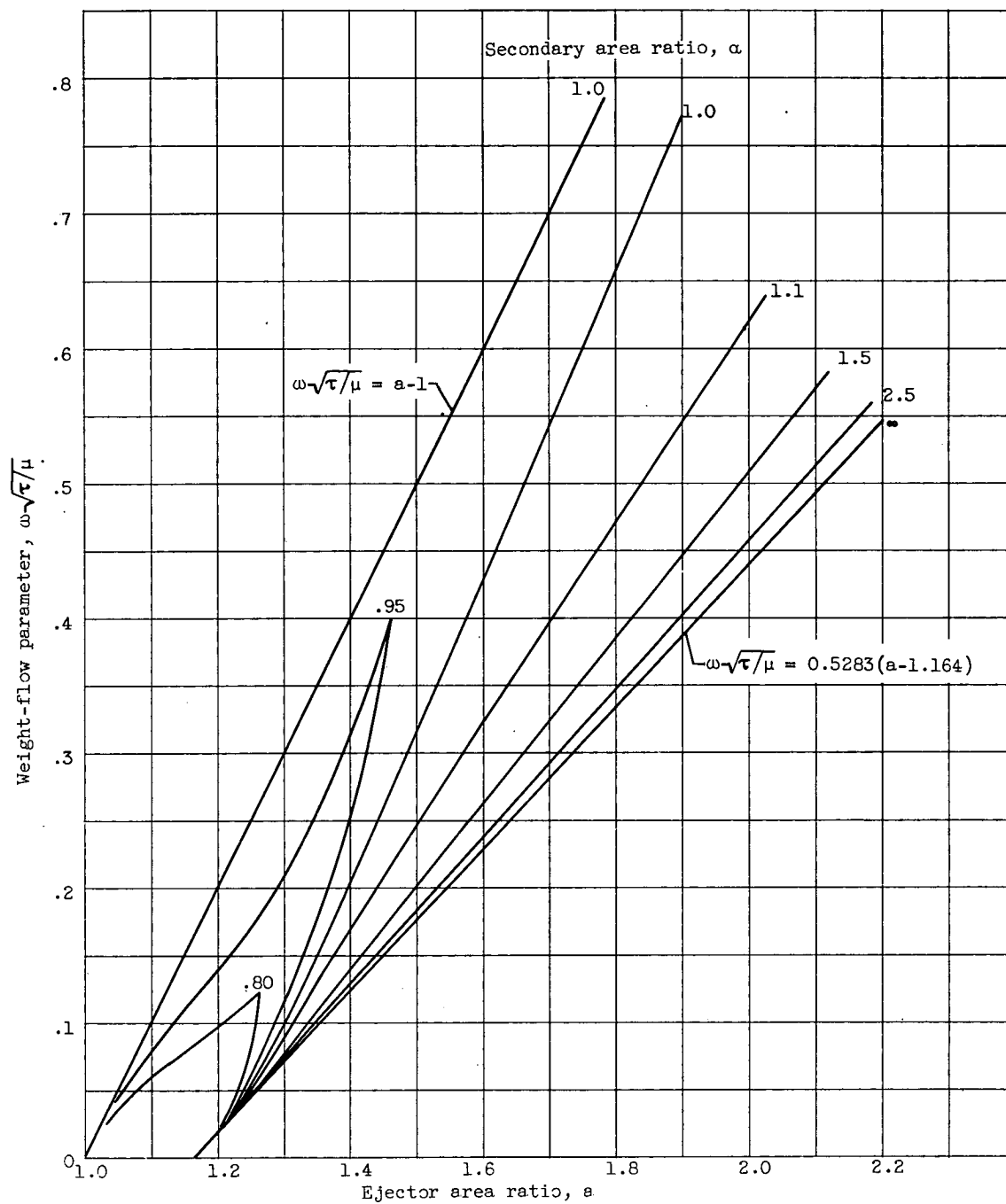
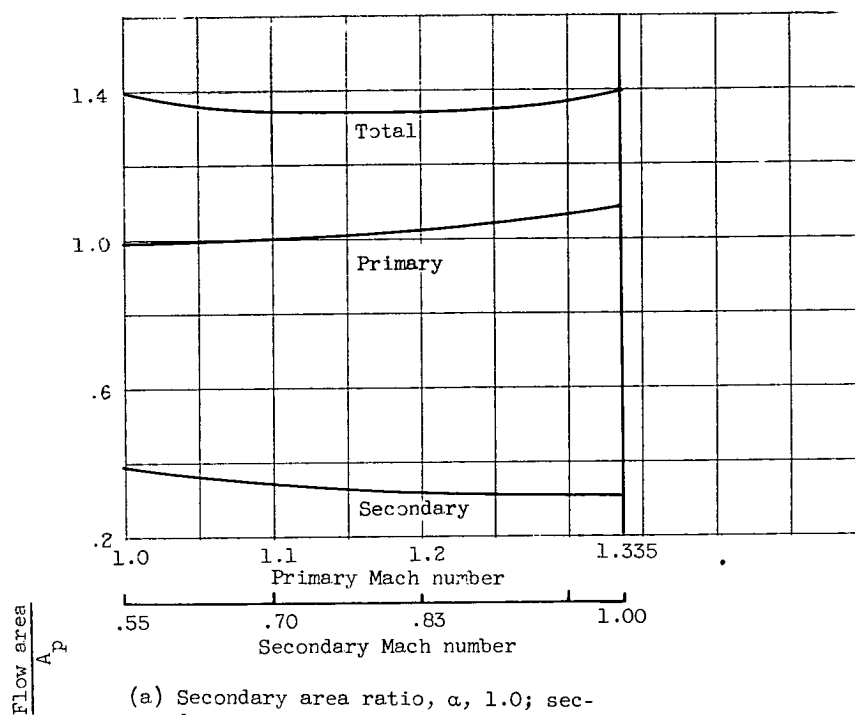
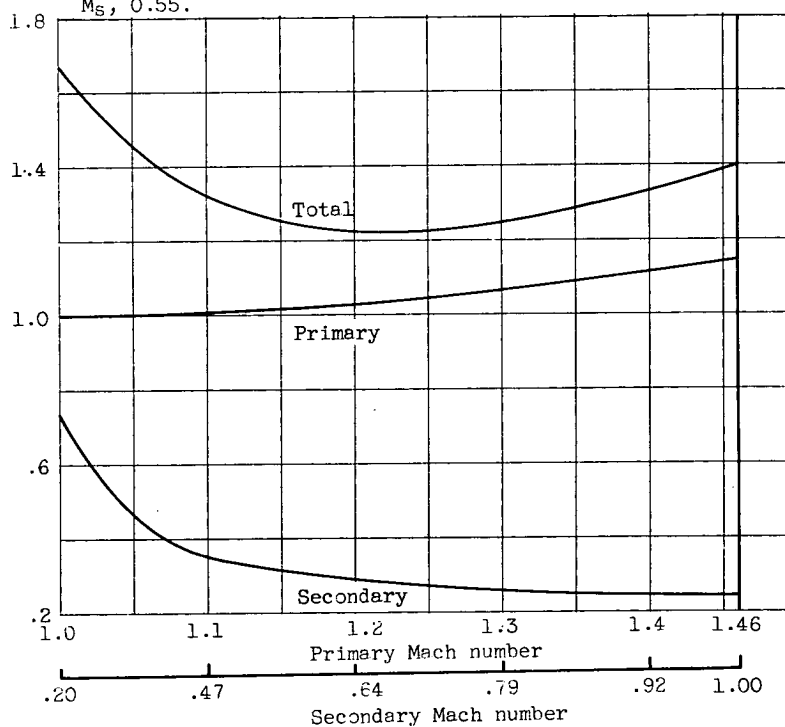


Figure 7. - Maximum weight flow for a choked primary nozzle. Primary Mach number, 1.0; nozzle discharge coefficient, 1.0.

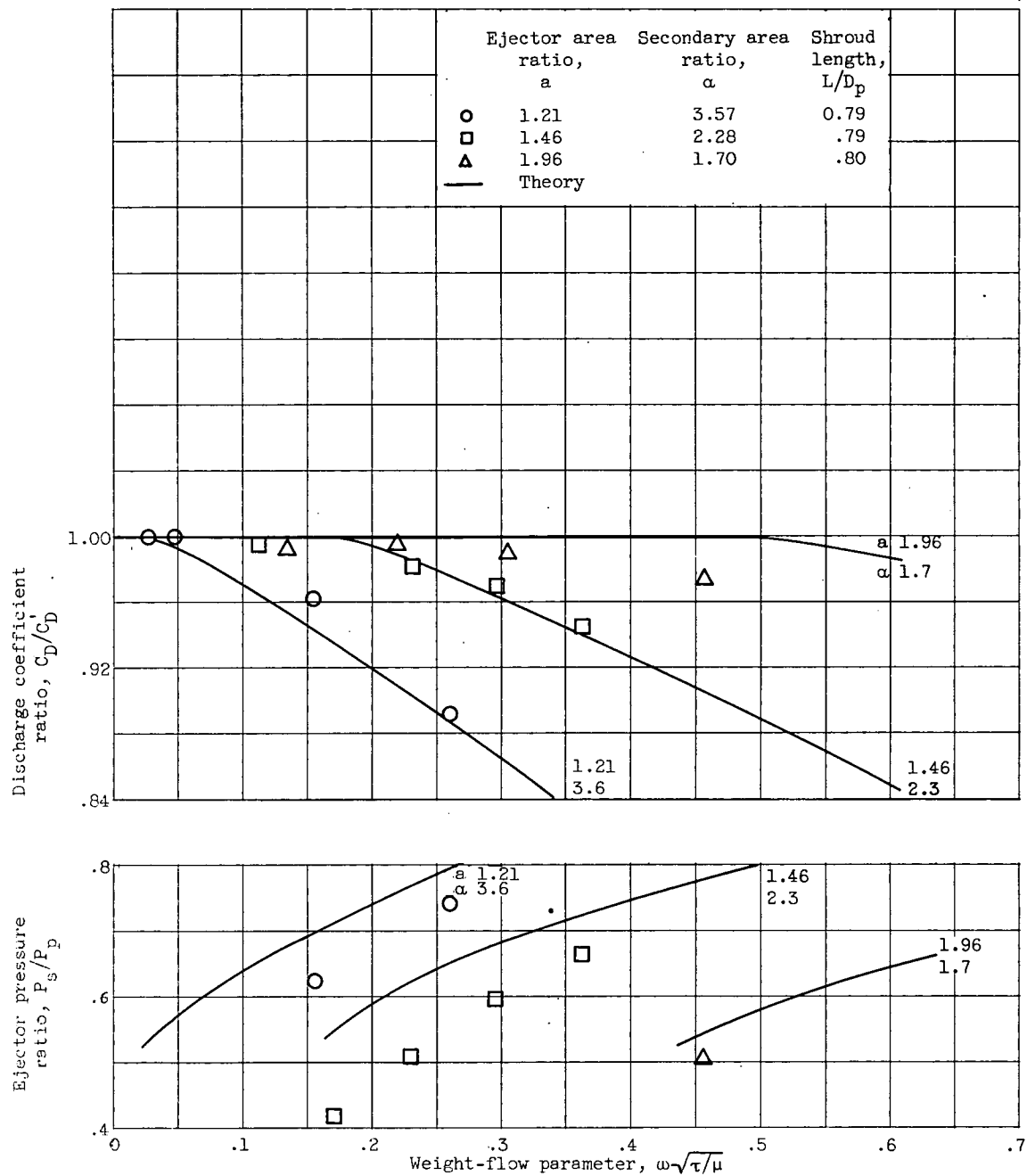


(a) Secondary area ratio, α , 1.0; secondary Mach number at nozzle exit, M_s , 0.55.



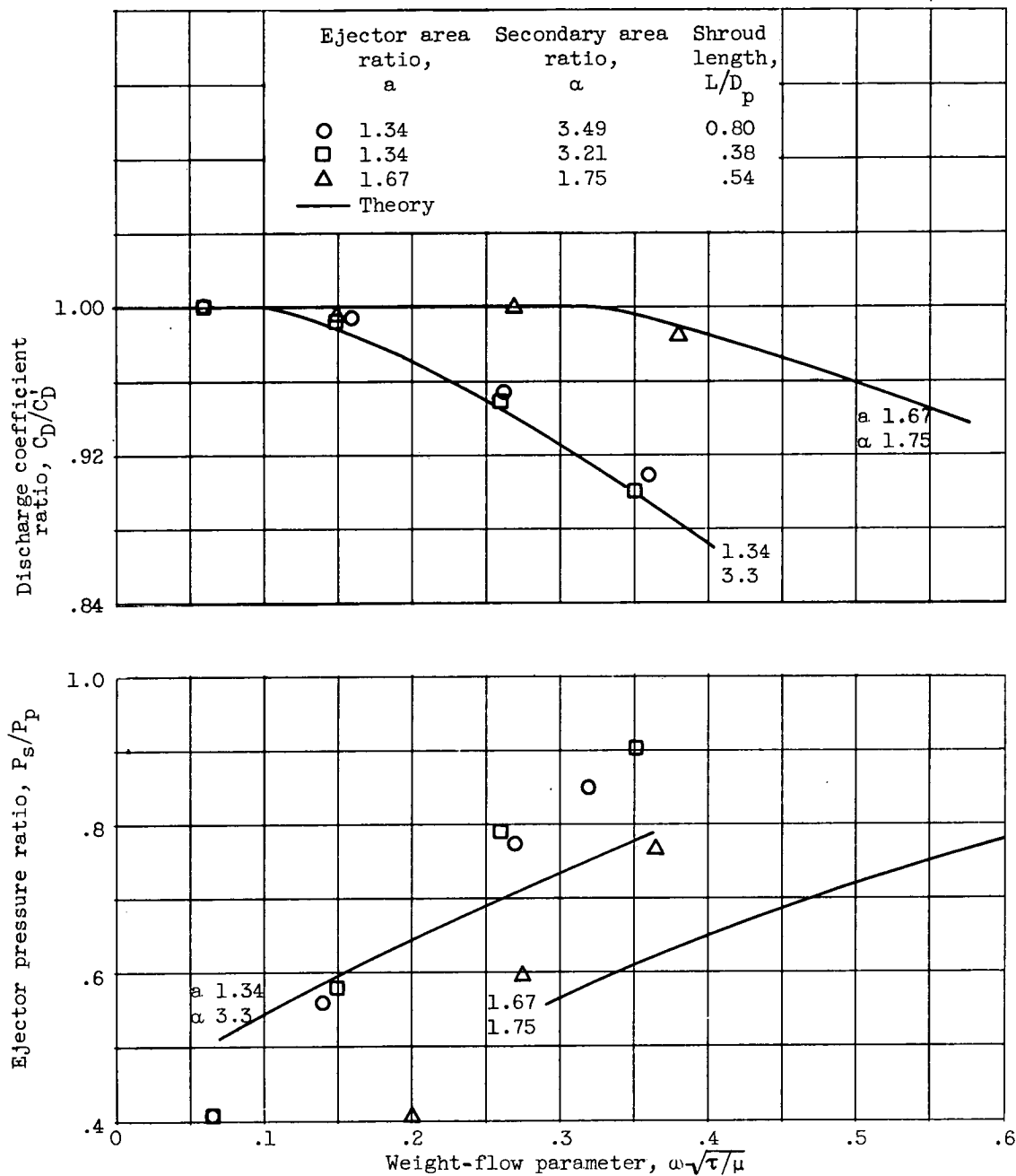
(b) Secondary area ratio, α , 1.85; secondary Mach number at nozzle exit, M_s , 0.20.

Figure 8. - Area distribution for isentropic flow.
Ejector area ratio, a , 1.4.



(a) Data from references 3 and 4.

Figure 9. - Comparison of theory and experiment for conical ejectors.



(b) Unpublished NACA data.

Figure 9. - Concluded. Comparison of theory and experiment for conical ejectors.

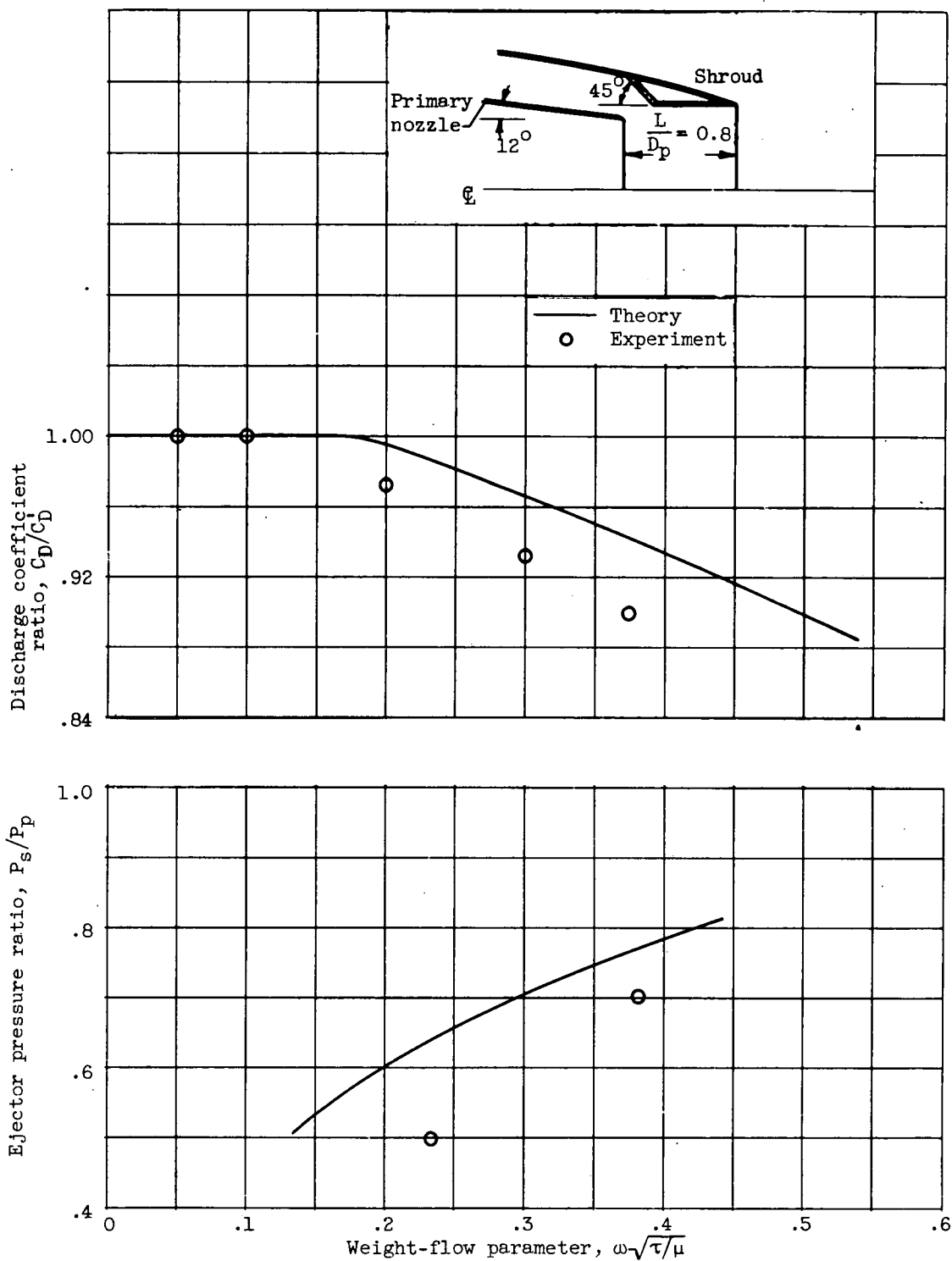


Figure 10. - Comparison of theory and experiment for semicylindrical ejector. Ejector area ratio, 1.44; secondary area ratio, 1.72. Data from reference 5.